931321

On the Dynamic Response of Hydraulic Engine Mounts

R. Matthew Brach and Alan G. Haddow
Michigan State Univ.

ABSTRACT

Hydraulic engine mounts are used in the automotive industry because they offer frequency and amplitude response characteristics superior to the conventional elastomeric engine mount. This response is well established but is not fully understood. Numerous articles have attempted to explain the complex behavior of these mounts using linear theory. This paper uses the same linear models developed in previous papers, but offers a more fundamental explanation of the system response using these previously derived two degree of freedom models. In addition, the source of engine vibrations and their corresponding frequency ranges are explained in detail. Techniques borrowed from control systems are used to interpret system response and terminology used in the automotive industry to describe the behavior of hydraulic engine mounts is clarified. Validation of the two degree of freedom model is made by comparison with experimental data.

INTRODUCTION

The engine-chassis-body system of automobiles is subjected to undesirable vibrational input from the engine and from the road and wheels. The engine excitation is typically in the range of 10 to 200 Hz. Wheel excitation is typically below 30 Hz. The design engineer has two means by which these vibrations can be eliminated. The first approach is to choose mount positions and characteristics such that a particular design criteria is met [1,2,3,4,5,6,7].* Two examples of these design criteria are: i) position the mounts such that the six rigid body vibrational modes of the engine are uncoupled from each other [1,4,5,6]; and ii) to select mount characteristics and positions such that natural frequencies are removed from frequencies of excitation [3,7]. The second approach to engine vibration isolation is to carefully design the mount to achieve the isolation characteristics appropriate for the frequencies and amplitudes of the vibration [8,9,11-21]. These isolation characteristics typically require the mount to exhibit the conflicting characteristics of large stiffness and large damping for the frequency range 1-30 Hz and low stiffness and low damping for frequencies of excitation above 30 Hz. These two approaches to engine vibration isolation are not mutually exclusive. Effective vibration isolation of an automobile engine requires proper placement of the appropriately designed mount.

This report employs the second approach to engine vibration isolation described above by focusing on the behavior of the class of engine mounts known as hydraulic engine mounts. The operation and response of these mounts is described in detail in this report. In particular, the dependence of the response of this type of mount on the frequency and amplitude of excitation permit the conflicting damping and stiffness characteristics mentioned above to be met.

The second section of this report is a comprehensive review of literature pertaining to hydraulic engine mounts. A detailed description of the source of engine vibration is described in the third section. In the fourth section the design and operation of an hydraulic engine mount are then discussed. In that section, the terminology used to describe the operating characteristics of hydraulic mounts is discussed and a linear two degree of freedom model is introduced to model their behavior. Interpretation of the dynamic stiffness of hydraulic engine mounts consistent with linear vibration theory is then presented. The report concludes with numerical verification of the two degree of freedom model through comparison of analytical results with experimental data.

*Numbers in brackets refer to references listed in the back of the paper.

LITERATURE REVIEW

The earliest mention of hydraulic mounts is found in Bernuchon's paper [9]. His report addresses a mount which uses a fixed-type decoupler.** He proposes a linear two degree of freedom system to model the mount but does not perform any analysis using this model. He establishes conventions used today to analyze hydraulic mounts, which are a nominal deformation amplitude of ±0.1mm for the frequency range 30-200 Hz and ±1.0mm for the frequency range 5-30 Hz. He defines complex dynamic stiffness in his report as the modulus of the ratio of the load transmitted to the frame to the input vibration amplitude. (More information will be presented later on the topic of dynamic stiffness.) He also uses the loss angle as the measure of the system damping. The loss angle is defined as the phase difference between the load transmitted by the mount and the input displacement. He presents experimental data which shows a 5dB reduction of noise levels inside the car due to the use of hydraulic engine mounts. Corcoran and Ticks [11] analyze several types of hydraulic mounts using a single degree of freedom model. They compare various configurations of mounts and show experimentally the range of performance that can be achieved using hydraulic mounts. They propose a decoupler to change the behavior of the mount. They give experimental results which show a general decrease in noise in the vehicle for hydraulic mounts versus elastomeric mounts. They demonstrate the effectiveness of the mount experimentally using a tuned mount to eliminate first order idle shake at 11 Hz. They also propose a criteria for the optimum placement of the hydraulic engine mount. In performing this optimization, the authors assume the maximum damping is achieved by stroking the mount through the vertical axis (see Figure 6) such that the inertia track is engaged. The mount provides little damping when stroked in shear since there is little movement of fluid for this motion. Flower [12] uses bond graphs to develop models of several different mount geometries. These models are used to explain the operation of the inertia track and the decoupler. He presents experimental data which shows the increased effectiveness of the hydraulic mount over the elastomeric mount. However, no direct comparison of the analytical model and experimental data is given. Clark [13] proposes a two degree of freedom mathematical model for a mount which has an inertia track but no decoupler. The parameters of the two degree of freedom model are modified to obtain two linear models for the two frequency ranges. He uses his models to perform tuning of parameters to provide desired force transmissibility in the low and high frequency ranges. He then incorporates this model into a three degree of freedom model representing one quarter of a car. Next, he proceeds to tune the mount for engine induced and road induced vibration obtaining optimum model parameters to minimize the displacement of one of the degrees of freedom. Marjoram [14] considers the use of hydraulic mounts for the isolation of tractor-trailer cabs. While this paper presents an interesting application, it also proposes the use of internal pressurization of the collector separator diaphragm (referred to as a bellow in Figure 6) for the accommodation of static load variations. This has the effect of tuning the hydraulic mount by changing its frequency response characteristics. Le Salver [15] presents experimental data for a mount with a free decoupler and also presents several theoretical models. However, no direct comparison of the analytical and experimental data is made. Sugino and Abe [16] develop a model of an hydraulic mount which uses an inertia track but no decoupler. They confirm the validity of the model with experimental results. They then consider a quarter car model incorporating their hydraulic mount model and compare this to experimental results. Ushijima et al [17,18] propose a two degree of freedom model and use it to evaluate the performance of hydraulic mounts to the superposition of a high frequency-low amplitude and low frequency-high amplitude input. They experimentally verify the ineffectiveness of the hydraulic mount with a free decoupler in isolating high frequency components. They attribute this to the heavy nonlinearity of the decoupler and they propose and alternative mount which uses a pliable fixed-type decoupler. The authors state that this alternative mount can provide a low dynamic stiffness for low forcing amplitude up to a frequency of 800 Hz.

Seto et al [19] model the hydraulic mount as a vibration absorber and uses optimization theory to minimize the ratio of the engine displacement to the frame displacement. The optimization method used is that presented by Hartog [20]. Experimentation is used to verify the models.

Nakajima, et al model the hydraulic engine mount using an hydraulic chamber model [22]. An expression for the ratio of the input force to the input displacement is derived using lumped parameters. This model is used in the design of an hydraulic strut mount [23]. In [23], correlation between analytical and experimental data for the hydraulic strut mount is presented.

The most recent and complete treatment of hydraulic mounts is given by Singh et al [21]. In this work, a linear time invariant model of the mount with inertia track and decoupler is developed using lumped mechanical and fluid elements. The model is validated experimentally for the frequency range 1 - 50 Hz. In this paper, parameter studies are performed, force transmissibility is investigated and comparisons to previous models are included. Model limitations are also discussed.

ENGINE VIBRATIONS

SOURCES AND FREQUENCY RANGES OF ENGINE VIBRATION - Vibrational excitation of the engine comes from two sources. One source is engine out of balance forces. For example, in a four cylinder in-line engine, out of balance

**A description of hydraulic mounts with free and fixed type decouplers is given later.

forces occur in the direction of piston motion at predominantly twice the crankshaft speed. These forces are called secondary or second-order forces and act in the vertical, or bounce direction. The lateral forces and primary forces in the vertical direction are completely balanced. For a complete discussion of the forces in multi-cylinder engines, see Hartog [20]. For an engine with a rotational speed range of 750 - 6000 rpm, the frequency of these out of balance forces is 25 - 200 Hz. Diesel engines pose special problems. These engines have unbalance forcing at half-order and first-order in addition to second-order forcing. These forces, due to uneven firing, and are mentioned in [8], but their source is not discussed.

The second source of engine excitation, road/wheel input, subject the vehicle chassis to inputs of both random and periodic form. Random inputs depend on the road surface and periodic inputs are due to wheel out of round or out of balance. These inputs can be amplified by resonances in the tire/suspension/chassis system. The predominant frequency range of these inputs is below 30 Hz.

Due to the nature of the two frequency ranges of engine vibration sources, the frequency range 1-200 Hz is typically separated into two ranges for engine mount analysis: 1-30 Hz and 30-200 Hz. It is important to note that the excitation below 30 Hz is associated primarily with wheel inputs. This excitation is transmitted from the wheel and suspension to the chassis such that the engine is forced from the base. The amplitudes of excitation in this frequency range are typically greater than 0.3mm. In the frequency range 30-200 Hz, the excitation is generated by the engine out of balance forces. The vibration amplitudes in this frequency range are generally less than 0.3mm.

ISOLATION OF ENGINE VIBRATIONS - In view of the amplitude and frequency ranges of the inputs to the engine, the fundamental problem of isolation of engine vibration becomes apparent. To isolate the engine out of balance forces, the engine should have a rigid body natural frequency below 30 Hz and usually in the 6-12 Hz range. This places the forcing frequency due to out of balance forces above these natural frequencies. Since the engine has six degrees of freedom, placing all the natural frequencies in this narrow range can be difficult. However, since the exciting force due to out of balance is primarily in the vertical direction, it is this natural frequency which is most significant. Therefore this frequency is kept in the 8-12 Hz range and the natural frequencies of the other modes are usually kept between 12 and 20 Hz. However, this means that the natural frequency of the vertical rigid body mode is in the range of the wheel input. Excitation of this mode from the frame input is known as engine shake. Similarly, excitation of the vertical mode from incompletely balanced first order engine forces can result and this is known as idle shake. This is usually perceived in the passenger compartment by vibration of the steering wheel and dashboard.

Single degree of freedom models can be used to understand the requirements of an engine mount to eliminate unwanted vibrations. The engine-mount system subjected to wheel inputs can be modeled as a mass supported on a spring and a dashpot. The mass represents the mass of the engine and the stiffness and damping characteristics of the mount are modeled as a spring and a dashpot respectively (see Figure 1). Second-order forces developed by the engine supported on mounts can be modeled as a mass supported by a spring and a dashpot with eccentric mass forcing (see Figure 3). The nondimensionalized displacement response, (X-Y)/Y, and the force transmissibility, F_T/F_o, for these two systems are given in Figures 2 and 4, respectively. The importance of these specific quantities will be given in the following discussion.

From previous considerations, a passive engine vibration control strategy can be established. Large amplitude rigid body vibrations resulting from wheel input in the 1-30 Hz range can be controlled using a mount with large stiffness and large damping. For this type of input, the base excitation system is used for analysis (see Figure 1). The relative displacement is examined since it is the motion of the engine on the mounts relative to the chassis which needs to be controlled. This control prevents the engine from encountering motion limiting stops and developing large forces. For large stiffness, the operating point on the response curve is to the left of r = 1 where the relative displacement is minimum. Increased damping increases the effectiveness regardless of the frequency ratio.

Lower stiffness and lower damping are needed to isolate the small amplitude vibrations resulting from unbalanced secondary forces. In this operating range, the system behaves as a single degree of freedom system with eccentric forcing. This system is shown in Figure 3 and response curves for the force transmissibility, F_T/F_o for various damping ratios are shown in Figure 4. The force transmitted to the chassis is examined since these forces result in transmission of acoustical noise to the passenger compartment. Isolation of these forces results in a quieter vehicle. For low stiffness, the operating point on the response curve is to the right of r = 1 where the transmissibility is less than 1. Decreased damping increases the effectiveness of the mount in this range.

Elastomeric mounts used in automobiles cannot satisfy these conflicting requirements for improved ride comfort and therefore hydraulic engine mounts have been developed. The stiffness and damping characteristics of these mounts vary with amplitude and frequency of excitation. Dynamic stiffness and loss angle response curves for a typical mount for the forcing amplitudes of 1.0mm and 0.1mm are shown in Figure 5.*** Ideally, the hydraulic engine mount should have large stiffness and have large damping for the frequency range 1 - 30 Hz and low stiffness and damping for the frequency range 30 - 200 Hz. The former frequency range corresponds to large forcing amplitudes from tire out of balance. For large forcing amplitudes the mount has large dynamic stiffness and therefore the

***A complete discussion of dynamic stiffness and loss angle will be given in later section.

displacements of the engine are reduced. The latter frequency range corresponds to low forcing amplitudes due to engine secondary forces. For these amplitudes the mount has low dynamic stiffness and therefore the force transmitted to the automobile frame is reduced. This decreases the acoustic transmission, sometimes called booming noise, to the passenger compartment. At very low frequency, the mount has low dynamic stiffness regardless of amplitude. The mount still performs adequately since no rigid body resonance appears in this frequency range. Table 1 presents concisely the operating ranges of the mount and the required characteristics discussed in this section.

HYDRAULIC ENGINE MOUNT DESIGN AND OPERATION

The performance of the hydraulic engine mount is described by analyzing the amplitude and frequency dependence of operation. Two approaches will be used for this description. The approach used in the first section is consistent with the descriptions given in automotive literature. In the following section more traditional means of describing system frequency response will be used. In the third section, comments regarding some of the previous explanations of hydraulic engine mount response characteristics are presented.

PHYSICAL GEOMETRY AND OPERATION - Figure 6 shows the typical geometry of an hydraulic engine mount with inertia track and free decoupler. For an hydraulic engine mount with a fixed type decoupler, the geometry shown in Figure 6 remains the same except that the decoupler is not free to move. Therefore no fluid is transferred between chambers A and B. Instead, a compliant membrane which deforms under pressure is used to restrict the flow of fluid through the decoupler channel. This action forces the engagement of the inertia track. The balance of this paper will be concerned with hydraulic mounts with a free decoupler. For small forcing amplitudes, (< 0.3mm is typical but the value can be varied by design), the fluid is free to move between chamber A and chamber B through the decoupler channel. In this mode of operation, the decoupler is suspended in the fluid and offers very little resistance to flow. The characteristics of the frequency response of the mount for this forcing amplitude are due primarily to the rubber housing. This mode of operation provides relatively low stiffness and damping which vary little with frequency up to 40 Hz.

Dynamic stiffness has been used as the frequency response function for hydraulic engine mounts in the automotive literature [8,9,11-21]. This dynamic stiffness is defined as the ratio of the force transmitted to the base mounting point to the input displacement. The phase associated with this complex ratio is called the loss angle and is often used incorrectly as an indication of the damping in the system [9,12]. Thus, for low amplitude vibrations, the hydraulic engine mount provides low dynamic stiffness magnitude and loss angle as shown in Figure 5. This results in low force transmissibility to the chassis and therefore reduced interior noise levels.

For large amplitude vibrations, (amplitudes > 0.3mm), the pumping action of the top chamber forces the decoupler to bottom on its seats terminating flow through the decoupler channel. The fluid flow resulting from the remainder of the input displacement is forced through the inertia track. This additional pumping of the mass of fluid in the channel together with the top and bottom compliances forms an oscillatory system. Thus for large amplitude input, the general nature of the dynamic stiffness plot is changed. The distinctive feature of the dynamic stiffness plot for large forcing amplitudes is the sharp increase in the magnitude of the dynamic stiffness at low frequencies. The loss angle also has a corresponding sharp increase (see Figure 5). These overall effects have been called inertia augmented damping [12,21].

APPLICATION OF LINEAR THEORY

Linear Time-Invariant Model - A fuller understanding of the operation of the hydraulic engine mount is provided by linear vibration theory using the linear time invariant model developed by Singh [21]. Figure 7 is a schematic representation of this lumped parameter model. For this model the "r" subscript refers to properties of the rubber and the "i" subscript refers to the properties of the inertia track. Hence m_r is the mass of the rubber and m_i is the equivalent mass if the fluid in the inertia track. The development of these model parameters from the hydraulic mount physical properties is given in [21]. This model applies to the coupled and decoupled states of the hydraulic mount through modification of k_1. To model the decoupled state, the value of k_1 must be set small and the inertia track is effectively uncoupled from the system. If the decoupler bottoms out, k_1 becomes significantly larger as the fluid then travels through the inertia track. Hence, with appropriate modification of parameters, this linear model can represent the two different operating regimes of the hydraulic mount. Often a simplified model is used to represent the mount under small stroke. In this case, only m_r, k_r and b_r are retained in what is often referred to as a voigt model for rubber. See [21] for further consideration of this topic.

Terminology - Prior to proceeding with the analysis of this system, qualification of the applicable frequency response functions is required. In [10], the admittance for a single degree of freedom system is defined as the ratio of applied force to displacement. The dynamic stiffness is defined as the reciprocal of the admittance. These quantities are further categorized for multi-degree of freedom systems as either point admittance or transfer admittance. A point response function is one in which the response and excitation are measured at the same system coordinate. A transfer response function is one in which the response and excitation are measured at separate system coordinates. ([21] refers to the transfer dynamic stiffness as the cross-point dynamic stiffness.) Note that the dynamic stiffness as defined and used with respect to hydraulic engine mounts measures the system response, in this case the force transmitted to the car frame, at a point which is not a system coordinate.

A comparison of point and transfer dynamic stiffnesses as used in the automotive and academic communities can be

easily made by considering an arbitrary system (see Figure 8). Table 2 lists the titles used by the automotive community and used in [10] for the system response quantities as depicted in Figure 8.

The difference in the point admittance and transfer admittance for the model in Figure 7 can also be seen in their analytical expressions. For the two degree of freedom system shown in Figure 7, the equations of motion are:

$$\begin{aligned} m_r\ddot{x}_r + b_r\dot{x}_r + (k_1 + k_r)x_r - k_1x_i &= F(t) \\ m_i\ddot{x}_i + b_i\dot{x}_i + (k_1 + k_2)x_i - k_1x_r &= 0 \end{aligned} \quad (1)$$

Transforming these two equations into the Laplace domain and performing the necessary algebraic manipulations, a transfer function for the point admittance is determined. This transfer function is:

$$\frac{X_r(s)}{F(s)} = \frac{m_is^2 + b_is + (k_1 + k_2)}{D} \quad (2)$$

where

$$\begin{aligned} D = {} & m_rm_is^4 + (m_rb_i + m_ib_r)s^3 + \\ & (m_r(k_1 + k_2) + b_rb_i + m_i(k_1 + k_r))s^2 + \\ & (b_r(k_1 + k_2) + b_i(k_1 + k_r))s + k_rk_1 + k_rk_2 + k_1k_2 \end{aligned}$$

In order to obtain an expression for the transfer admittance, the equation for the force transmitted to the base is required. This equation is:

$$F_T = k_rx_r + b_r\dot{x}_r + p_A(t)A_r \quad (3)$$

The pressure in chamber A (see Figure 6), p_A, has been included in the force at the base since a portion of this force has been transmitted by p_A acting on the internal decoupler support structure. An expression for the pressure in terms of the lumped parameters of the equivalent mechanical system is obtained through equations presented in [21]. The resulting transfer function for the transfer dynamic stiffness is:

$$\frac{X_r(s)}{F_T(s)} = \frac{m_is^2 + b_is + (k_1 + k_2)}{D} \quad (4)$$

where

$$\begin{aligned} D = {} & m_rm_is^4 + (m_rb_i + m_ib_r)s^3 + \\ & (m_r(k_1 + k_2) + b_rb_i + m_i(k_1 + k_r))s^2 + \\ & (b_r(k_1 + k_2) + b_i(k_1 + k_r))s + k_rk_1 + k_rk_2 + k_1k_2 \end{aligned}$$

$X_r(s)$ is the Laplace domain representation of the input displacement $x_r(t)$. $F(s)$ and $F_T(s)$ are the Laplace domain representations of the forces measured at the input and the output, respectively, where the output force is measured at ground. The complex frequency response function of the system is found by replacing s with jω in EQ (2) and (4) and if required, the magnitude and phase may be determined in the usual manner.

The qualitative shape of frequency response functions can be understood by looking at the poles and zeros in the complex plane. To do this, first s is replaced by jω in EQ (2) and (4). The resulting polynomials in ω in the numerator and denominator can be factored into their individual roots. These individual factors can be interpreted as vectors that originate at the pole or zero and terminate at jω. As ω varies from zero to infinity along the positive imaginary axis, the length of the vectors change accordingly. In considering the magnitudes of the individual vectors as ω changes, the magnitude of the overall frequency response function can be determined. For example, if the length of a vector emanating from a pole becomes very small, the magnitude of the frequency response will become very large.

Figure 9 depicts the complex plane with three poles (x's) and two zeros (o's) which is representative of a transfer admittance frequency response function. The general shape of the response function can be seen by using the method just described. Poles near the imaginary axis give large response at the frequency equal to the magnitude of the imaginary part of the pole. The frequencies at which these occur are the resonance frequencies. Zeros close to the imaginary axis will have the opposite effect, causing the admittance to become small, resulting in an antiresonance [10]. If the frequency response function has no zeros, no antiresonances appear.

For the point admittance, the response curve has two resonance peaks corresponding to the two pairs of complex conjugate poles, and one antiresonance peak corresponding to the one pair of complex conjugate zeros. The frequency of the antiresonance will always appear between resonance frequencies [10]. For the transfer admittance, one of the complex conjugate pairs of poles becomes a real pole and one of the resonant peaks disappears. The disappearance of one of the resonance peaks is a result is a result of the location of the measurement point not being a system coordinate. For the transfer admittance, a resonant type response may appear near ω=0 if the real pole is very near the imaginary axis. The antiresonance due to the complex conjugate zeros of the transfer function remains. From this analysis, it can be ascertained that for a given set of system parameters and the definition of transfer admittance given above, the location of the resonance frequencies need not be the same for the point and transfer admittances. Indeed, they are likely to be different, with the most notable difference that the transfer admittance will have only one resonance peak. The location of the antiresonance will remain the same as this depends only on the zeros of the transfer function, which are the same for both point and transfer admittance transfer functions. Differences in the phase of the frequency response will also be seen as a result of the difference in the location of the poles and zeros. Modification of the system parameters serves to move the poles and zeros in the complex plane. The system response can be tuned accordingly.

Interpretation of Dynamic Stiffness - The general features of the magnitude of the dynamic stiffness and loss angle plots for

Table 1

Frequency Range of Operation	Less than 30 Hz	30 Hz to 200 Hz
Vibrational Source	Wheel out of balance and out of round.	Engine secondary forces.
Amplitude Range	Large: > 0.3mm	Small: < 0.3mm
Operational Requirement of the mount	Large stiffness and large damping.	Low stiffness and low damping.

the hydraulic engine mount under large amplitude excitation can now be explained. Referring to Figure 5, it can be seen that as the forcing frequency is increased from zero to 40 Hz along the x-axis, the response initially drops slightly then quickly rises to a maximum before settling down to a constant value. The first dip at around 8 Hz is due to a damped resonance. Recall that for dynamic stiffness, resonances are a consequence of zeros and antiresonances are a consequence of the poles of the transfer function. These create dips and peaks in the magnitude response, respectively. This is opposite to the convention typically used for magnitude response plots of vibratory systems in textbooks. The first dip of the transfer dynamic stiffness at about 8 Hz is due to the set of complex conjugate zeros of the dynamic stiffness transfer function. The sharp increase in dynamic stiffness is due to the appearance of a pole in the denominator of the transfer function. This appears as a well damped antiresonance. The stiffness then remains relatively constant up to 40 Hz. The remaining zero s real and is typically located in the far left half-plane. Its effect is to generally decrease the influence of the zeros of the numerator of the transfer function, smoothing out the response curve. This affect can be seen in Figure 5. If less damping were present in the system, sharper peaks would be seen for the resonance and the antiresonance.

The profile of the loss angle, or phase of the dynamic stiffness, can be similarly explained. First consider this transfer function with no damping. For this case, all the complex conjugate poles and zeros are located on the imaginary axis. The remaining real zero is effectively moved to negative infinity. It then has negligible influence on the phase for small ω. For this case the phase will begin at zero and change by $+\pi$ at the resonance frequency. A change of $-\pi$ occurs at the antiresonance bringing the phase to zero where it remains. This creates a square pulse shaped phase response. As the damping is increased, the sharpness of the changes in phase is diminished. For large damping, and in this instance for a low resonance frequency, the phase becomes nonzero for small frequencies. After passing through the resonance frequency the phase comes under the influence of the antiresonance which begins to decrease the phase. After passing through the antiresonance, the phase slowly approaches zero as the forcing frequency is increased.

Comments on Terminology used to Describe Hydraulic Mounts - Terminology used previously to explain plots of dynamic stiffness can now be examined. The term "loss angle" in reference to the phase of the dynamic stiffness is not accurate. This name seems to have been adopted as it was thought that the increase in phase for large amplitude forcing was an indication of the damping in the system. The characteristic increase and decrease in the phase is due to the fact that the response is for a two degree of freedom system. The peak of the phase response would be larger if less damping were present in the system.

The phrase "inertia augmented damping" has also been used in reference to the response of the hydraulic engine mount for large amplitude forcing [12,21]. In [12] it is correctly indicated that damping alone is not adequate in explaining the phase relationship of the input displacement and the transmitted force of the mount under large amplitude input. Hence, the author recommends the phrase "inertia augmented damping". However, with the explanation of the response given in the previous section, "inertia augmented damping" is not an accurate description. The response is described accurately using linear theory.

NUMERICAL VALIDATION OF THE LINEAR TIME-INVARIANT MODEL

Using EQ (4), a comparison of data obtained experimentally from an hydraulic engine mount and the linear analytical model can be made. Figures 10 and 11 show a comparison of the experimental and analytical magnitude and phase of the transfer dynamic stiffness, respectively. For both the magnitude and the phase, very good correlation is seen over the frequency range 0-40 Hz. The parameters used for the analytical model were found using an optimization routine which minimized the sum of the magnitudes of the difference between the experimental and analytical complex dynamic stiffness values over the frequency range of the experimental data, 0-40 Hz. The parameter values used to produce the analytical results shown in Figures 10 and 11 were found by setting the parameter k_2 to zero prior to the optimization. k_2 represents the spring constant associated with the collector separator diaphragm for chamber B (see Figure 6). This diaphragm is very compliant in comparison to k_1 and k_r, so this assumption is reasonable. The parameter values given by the optimization and used for this analysis are:

Table 2

Mathematical Expression	Automotive Community	Ewins [10]
$X(s)/F(s)$	Not used	Point Admittance
$F(s)/X(s)$	Not used	Point Dynamic Stiffness
$X(s)/F_T(s)$	Not used	Transfer Admittance*
$F_T(s)/X(s)$	Dynamic Stiffness	Transfer Dynamic Stiffness*

*The definitions from [10] require that all response quantities be measured at a system coordinate. Here, F_T is not measured at a system coordinate.

k_r = 181238.0
k_1 = 77108.1
k_2 = 0.0
b_r = 115.5
b_i = 1224.3
m_i = 16.9

Using the parameter values determined in the optimization, the poles and zeros of the transfer function for the transfer dynamic stiffness were found. The three zeros are:

$s_{1,2} = -36.53 \pm i43.20$ $\quad$ $s_3 = -2235.86$

The poles of the transfer function are:

$s_{1,2} = -36.21 \pm i57.01$

These pole and zero locations are consistent with the complex plane mapping technique outlined previously.

Similar results to those just presented are given in [21]. In [21], a (2^{nd} order)/(2^{nd} order) transfer function with $b_r = 0$ is used. It is assumed that $k_1 >> 100k_2$. The results presented in [21] using this simplified transfer function, entitled the Reduced Order Form of Model II, could not be duplicated using the optimization technique described above. Determination of the parameters using the optimization technique with the transfer function as given in EQ (4) with all six parameters free, yielded physically unrealizable results. Similar unrealistic results were obtained by optimizing EQ (4) with only $b_r = 0$.

CONCLUSIONS AND COMMENTS

This paper explains the operation and response of hydraulic engine mounts in detail. In doing so, the sources and characteristics of engine vibrations are thoroughly discussed. The means by which hydraulic engine mounts meet the requirements for improved engine isolation is explained using linear vibration theory. Verification of the use of a linear, damped two degree of freedom model to predict the response of the mount for large amplitude forcing was done.

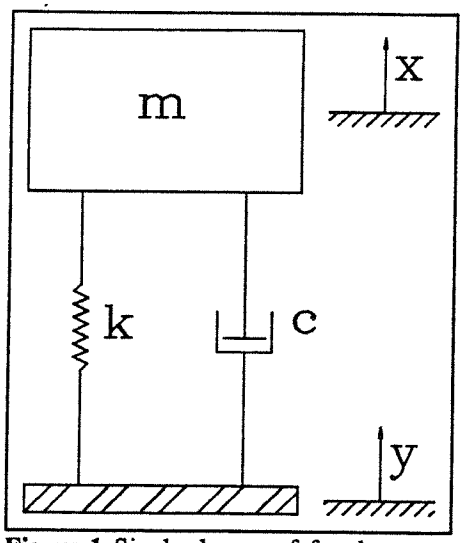

Figure 1 Single degree of freedom system undergoing base excitation.

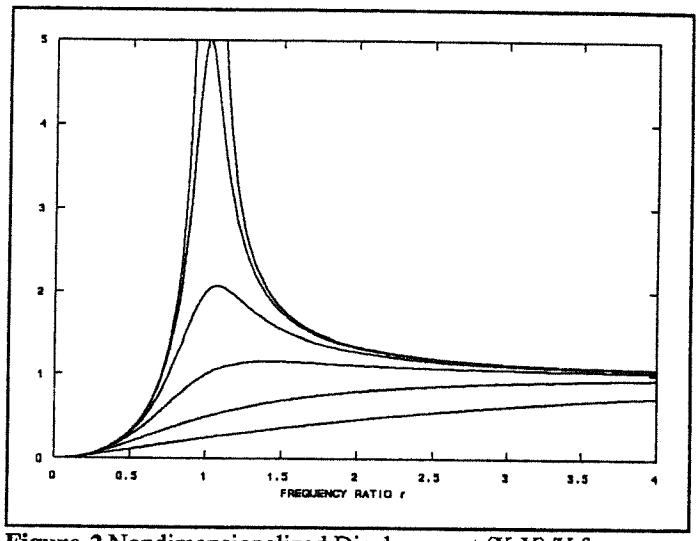

Figure 2 Nondimensionalized Displacement (X-Y)/Y for system under base motion. (Frequency ratio $r = \omega/\omega_n$)

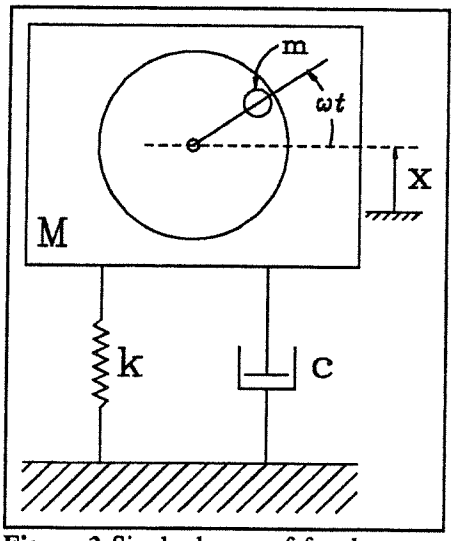

Figure 3 Single degree of freedom system undergoing eccentric mass excitation.

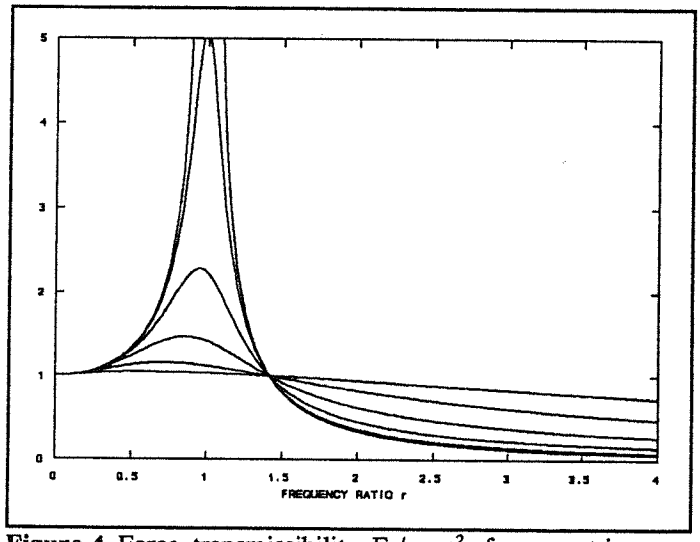

Figure 4 Force transmissibility $F_T/me\omega^2$, for eccentric mass system. (Frequency ratio $r = \omega/\omega_n$)

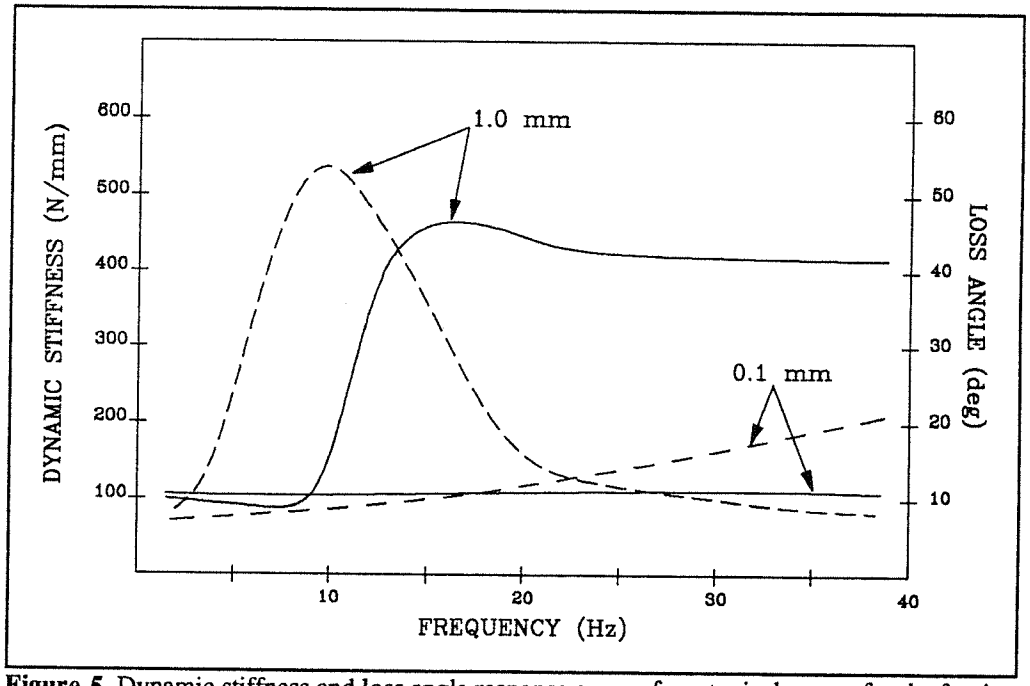

Figure 5 Dynamic stiffness and loss angle response curves for a typical mount for the forcing amplitudes of ±1.0mm and ±0.1mm.

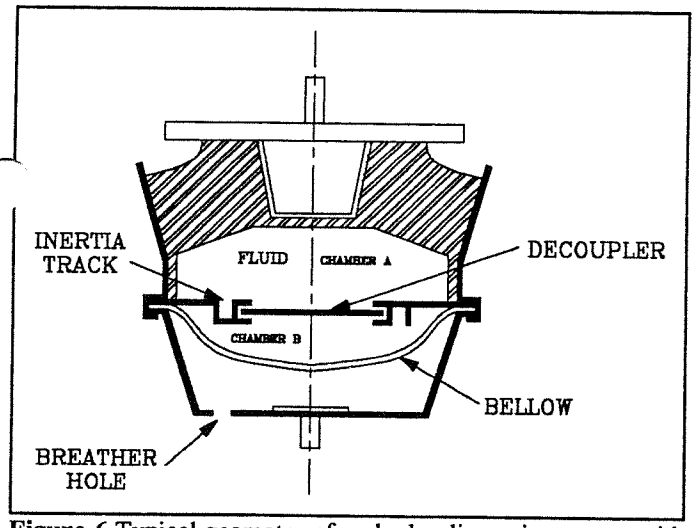

Figure 6 Typical geometry of an hydraulic engine mount with inertia track and free decoupler.

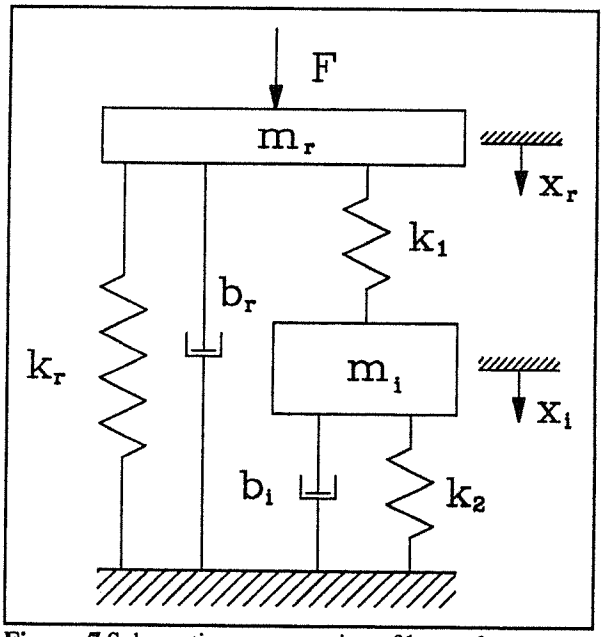

Figure 7 Schematic representation of lumped parameter two degree of freedom model of an hydraulic engine mount.

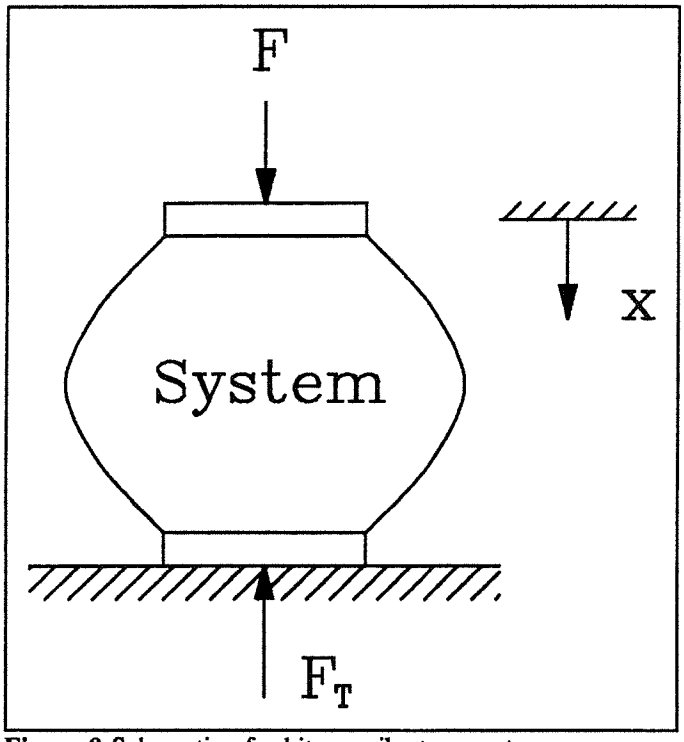

Figure 8 Schematic of arbitrary vibratory system.

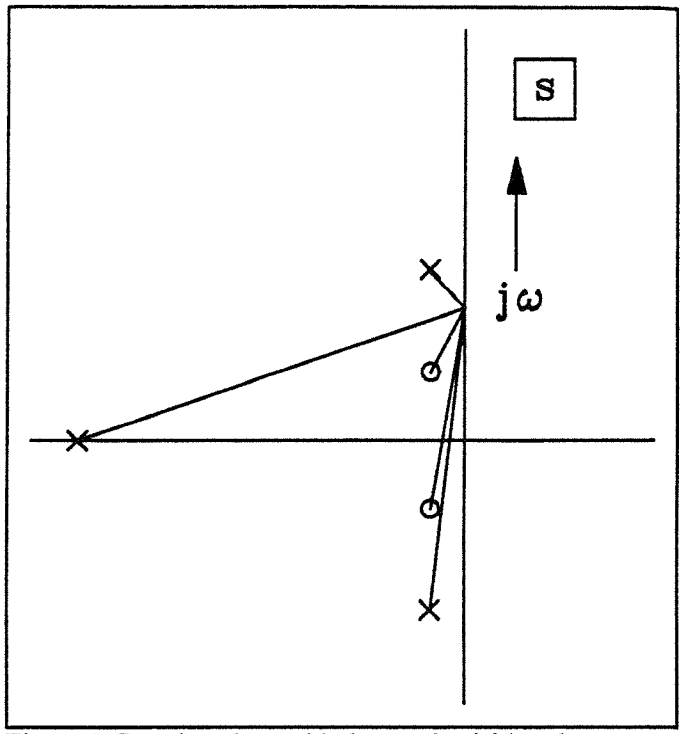

Figure 9 Complex plane with three poles (x's) and two zeros (o's) representative of a transfer admittance frequency response function.

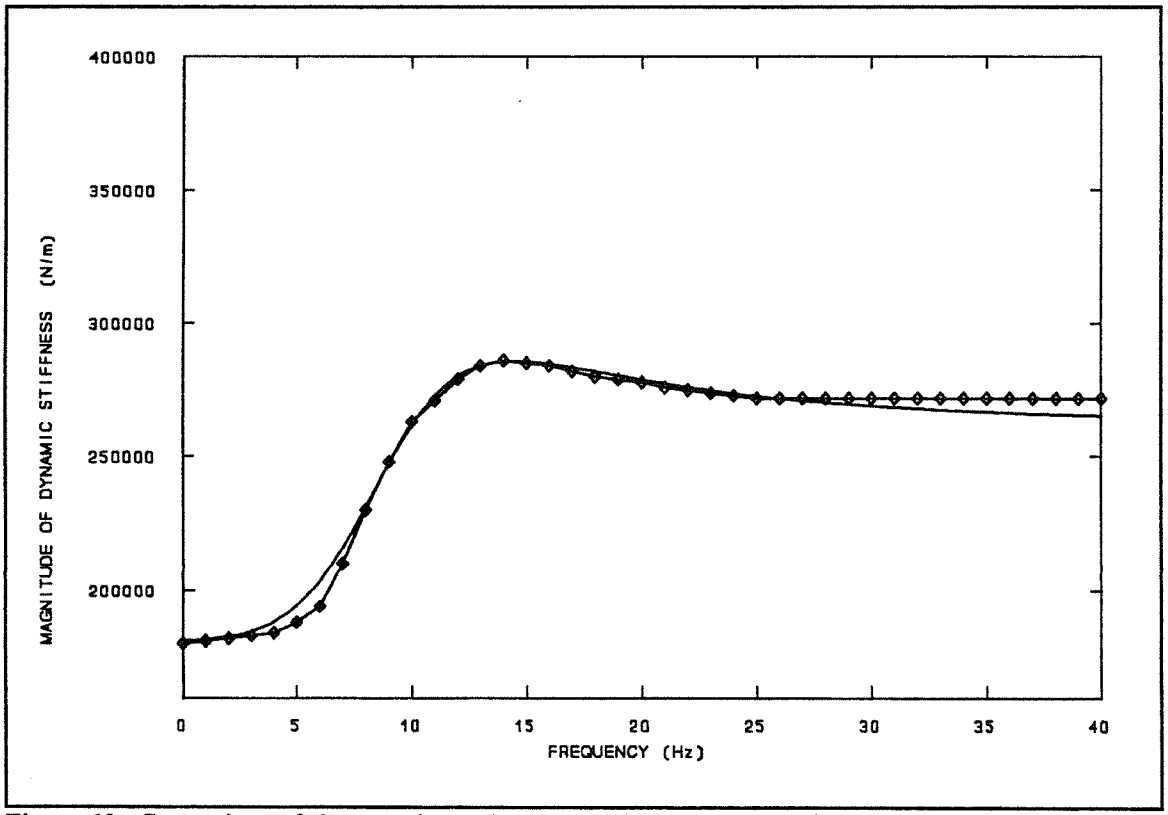

Figure 10 Comparison of the experimental and analytical magnitude of the transfer dynamic stiffness. Experimental data given by ◇.

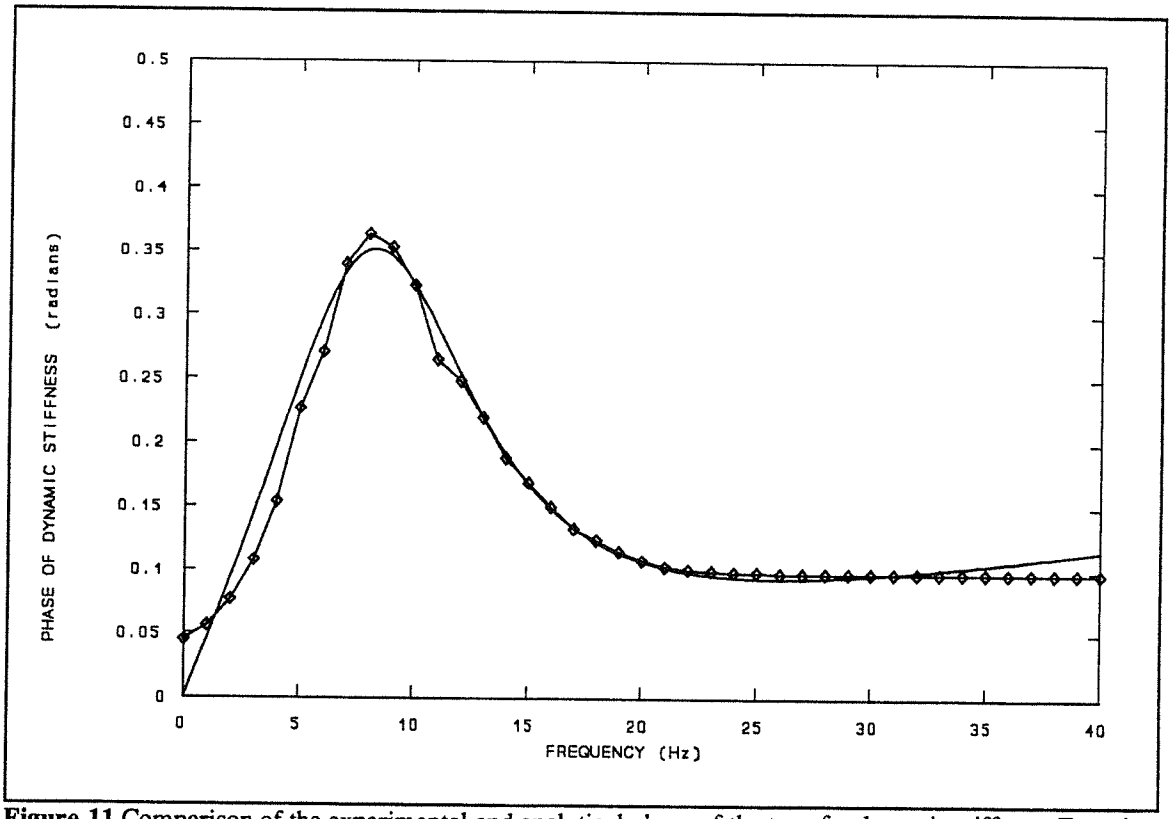

Figure 11 Comparison of the experimental and analytical phase of the transfer dynamic stiffness. Experimental data given by ◇.

REFERENCES

1. Timpner, Fred F., Design Considerations for Engine Mounting, (966B) SAE Paper 650093
2. Johnson, Steven. R. and J. W. Subhedar, Computer Optimization of Engine Mount Systems, SAE Paper 790974.
3. Bernard, James E. and John M. Starkey, Engine Mount Optimization, SAE Paper 830257.
4. Radcliffe, Clark J., Mark N. Picklemann, Charles Spiekermann and Donald S. Hine, Simulation of Engine Idle Shake Vibration, SAE Paper 830259.
5. Geck, P. E. and R. D. Patton, Front Wheel Drive Engine Mount Optimization, SAE Paper 840736.
6. Ford, David M., An Analysis and Application of a Decoupled Engine Mount System for Idle Isolation, SAE Paper 850976.
7. Hata, H., and H. Tanaka, Experimental Method to Derive Optimum Engine Mount System for Idle Shake, SAE Paper 870961.
8. West, J. P., Hydraulically-damped engine-mounting, Automotive Engineer, 12(1), 17-19, 1987.
9. Bernuchon, Marc, A New Generation of Engine Mounts, SAE Paper 840259.
10. Ewins, D. J., Modal Testing: Theory and Practice, Research Studies Press Ltd., Letchworth, Hertfordshire, England, 1986.
11. Corcoran, Patrick E.,& Gerd-Heinz Ticks, Hydraulic Engine Mount Characteristics, SAE Paper 840407.
12. Flower, Wallace C., Understanding Hydraulic Mounts for Improved Vehicle Noise, Vibration and Ride Qualities, SAE Paper 850975.
13. Clark, M., Hydraulic Engine Mount Isolation, SAE Paper 851650.
14. Marjoram, Robert H., Pressurized Hydraulic Mounts for Improved Isolation of Vehicle Cabs, SAE Paper 852349.
15. Le Salver, R., The use of engine mounts with integrated hydraulic damping in passenger cars, International Journal of Vehicle Design, vol. 7, no. 1/2, 1986.
16. Sugino, Marsaru and Eiichi Abe, Optimum Application for Hydroelastic Engine Mount, SAE Paper 861412.
17. Ushijima, Takao and Takuya Dan, Nonlinear B.B.A. for Predicting Vibration of Vehicle with Hydraulic Engine Mounts, SAE Paper 860550.
18. Ushijima, Takao, Kazuya Takano and Hiroshi Kojima, High Performance Hydraulic Mount for Improving Vehicle Noise and Vibration, SAE Paper 880073.
19. Seto, Kazuto, Katsumi Sawatari, Akio Nagamatsu, Masao Ishihama and Kazuhiro Doi, Optimum Design Method for Hydraulic Engine Mounts, SAE Paper 911055.
20. Den Hartog, J. P., Mechanical Vibrations, Dover Publications, New York, 1985.
21. Singh, R., Kim, G., Ravindra, P.V., Linear Analysis of an Automotive Hydro-Mechanical Mount with Emphasis on

Decoupler Characteristics, Journal of Sound and Vibration(1992) **158**(2), 219-243.
22. Nakajima, Z., and S. Ito, Study of Hydraulic Engine Mount Characteristics, JSAE Paper 861042, in Japanese.
23. Nakajima, Z., C. Matsuoka and S. Okuya, The Development of Hydraulic Strut Mount, SEA Paper 901729.